ISAS/EP/97/85

Reflection Scattering Matrix of the Ising Model in a Random Boundary Magnetic Field[1]

A. De Martino[a,b], M. Moriconi[c] and G. Mussardo[a,b,c]

[a] *International School for Advanced Studies, Via Beirut 2-4, 34014 Trieste, Italy*
[b] *Istituto Nazionale di Fisica Nucleare, Sezione di Trieste*
[c] *International Centre for Theoretical Physics*
Strada Costiera 11, 34014 Trieste,Italy

Abstract

The physical properties induced by a quenched surface magnetic field in the Ising model are investigated by means of boundary quantum field theory in replica space. Exact boundary scattering amplitudes are proposed and used to study the averaged quenched correlation functions.

[1] Work done under partial support of the EC TMR Programme *Integrability, non–perturbative effects and symmetry in Quantum Field Theories*, grant FMRX-CT96-0012

1 Introduction

There has recently been increasing interest in the exact estimations of boundary effects in statistical models and quantum field theories, following seminal works by Cardy based on conformal invariance [1] as well as a pioneering paper by Ghoshal and Zamolodchikov [2], based on the integrability of the boundary interaction[1]. New results have been obtained in many subjects, as for instance, the subjects of quantum impurity problems and dissipative quantum mechanics [6, 7, 8] or the exact calculation of correlation functions and Casimir energy in the presence of boundary conditions [1, 9, 10, 11]. Aim of this paper is to enlarge the range of applicability of boundary field theory to systems which present boundary effects induced by a quenched surface disorder and to propose an exact non–perturbative approach based on boundary scattering theory[2]. The model considered here is the two–dimensional Ising model in the euclidean half–plane $\Gamma = \{(x, y) \in \mathbf{R}; x \geq 0\}$ with a random magnetic field coupled only to the boundary spins. This model was previously investigated by renormalization group techniques and conformal field theory methods in [15, 14]. Its dynamics may be described by the euclidean action

$$\mathcal{A} = \mathcal{A}_0 + \int_{-\infty}^{+\infty} dy\, h(y)\sigma(y) \ , \tag{1.1}$$

where $\mathcal{A}_0$ is the bulk action relative to the Ising model in its high–temperature phase in a half–space geometry, with free boundary conditions adopted at $x = 0$. In eq. (1.1) $\sigma(y)$ is the local boundary magnetic operator and $h(y)$ is a quenched random field with Gaussian distribution of mean $\bar{h}$ and variance Δ:

$$\overline{h(y)} = \overline{h} \quad ; \quad \overline{h(y_1)h(y_2)} = \overline{h}^2 + \Delta\, \delta(y_1 - y_2) \ . \tag{1.2}$$

In the bulk, the massive excitation of the model may be regarded as an interacting bosonic particle $A(\theta)$ created by the magnetization operator[3]. Its elastic S-matrix is simply given by $S = -1$ [18]. The case $\Delta = 0$ corresponds to the usual Ising model with boundary magnetic field, which was originally discussed by Ghoshal and Zamolodchikov [2]: these authors proved that the model is integrable and therefore all its properties (as for instance, its partition functions and its correlators [9, 10]) can be recovered by using both its exact 2–body S-matrix in the bulk and the elastic boundary scattering matrix

[1] See also [3] for boundary scattering theory and refs. [4, 5] for a general introduction to boundary effects.

[2] We refer the reader to the references [2, 16, 17] for all details and notations relative to exact boundary and bulk S–matrices.

[3] As usual, θ is the rapidity variable which parameterises the dispersion relations $(E, p) = (m\cosh\theta, m\sinh\theta)$ of the particle.

given by

$$\mathcal{R}(\theta,\bar{h}) = i\tanh\left(\frac{\theta}{2} - \frac{i\pi}{4}\right)\frac{i\sinh\theta - \kappa}{i\sinh\theta + \kappa}\ , \tag{1.3}$$

where $\kappa = 1 - \frac{\bar{h}^2}{2m}$.

In terms of microscopic processes, the scattering event is nothing else but the result of an infinite number of interactions which take place on the boundary and which enter the self–energy of particle A, each of these interactions involving the insertion of the magnetic field h (see for instance Fig. 1.a for a graph of order h^6). The integrability of the model means that all scattering processes at the boundary proceed without particle production or absorption, i.e. an observer will always see a particle arriving at the boundary and bouncing back.

The graph technique can be also used to account for the interaction due to the random fields. The only new feature is that we have to average over the random variables $h(y)$, an operation which is performed[4] by using eqs. (1.2). This can be graphically represented by pairing by means of dotted line the small circles which represent the magnetic fields (see for instance Fig. 1.b), each of which gives a factor Δ. These extra terms will certainly increase the intricacy of the self–energy of the particle propagator but they cannot spoil the integrable nature of the boundary magnetic interaction, i.e. the one–to–one nature of the scattering process of the particle which hits the boundary. The reason is that the graphs which result from the average are similar to those entering the pure system which are integrable. Hence, we conclude that the dynamics associated with the Ising model with quenched boundary magnetic field may also be described by an integrable model.

This paper is organised as follows: in Section 2 the model is formulated in the replica space and the exact reflection S–matrix is computed. In Section 3 we compute some quenched averaged correlation functions using the exact scattering theory. In Section 4 we apply the Thermodynamical Bethe Ansatz to compute boundary entropies. Our conclusions are in Section 5.

2 Boundary scattering in replica space

The quenched averages of the disordered systems can be obtained by using the so–called replica trick which is based on the identity $\overline{\log Z} = \lim_{n\to 0}(\overline{Z^n} - 1)/n$, where $\log Z$ is the free energy of the model under investigation. In this way the original random problem is mapped onto a quantum field theory problem, described by an effective action involving n degrees of freedom in the limit $n \to 0$. Apart from subtleties in taking the $n \to 0$ limit,

[4]It may be convenient to separate the contributions which originate from the average value $\bar{h}$ by redefining $h(y) \to h(y) - \bar{h}$.

the advantage of this transformation is that it makes available to us powerful tools of quantum field theory and therefore opens up a way of obtaining non–perturbative results on the original random system. For the problem of interest in this paper, it is easy to see that by using (1.2), the effective action is given by

$$\begin{aligned} \mathcal{A}^{(rep)} &= \sum_i \mathcal{A}_0^{(i)} + \overline{h} \int_{-\infty}^{+\infty} dy \sum_a^n \sigma_a(y) \\ &\quad - \Delta \int_{-\infty}^{+\infty} dy \sum_{a<b}^n \sigma_a(y)\, \sigma_b(y) \ . \end{aligned} \tag{2.1}$$

The action (2.1) describes n copies of the Ising model hinged together at the boundary (Fig. 2). In addition to the coupling to the (mean) boundary magnetic field, the new interaction in the action (2.1) describes a process where a particle with replica index a arrives at the boundary and then changes to a particle with another label b. This elementary process may be repeated along the boundary an arbitrary number of times until the particle is finally re-emitted. Since no production events are involved, the boundary action (2.1) defines to a boundary integrable theory. In the following we will assume the validity of the above argument irrespective of the actual value of n, in particular also for the values $n < 2$. Consequently, there are two possible channels the elastic reflections $\mathcal{R}_{ab}(\theta)$ can go through: (1) the first channel is the reflection process described by the amplitude $P(\theta)$ where the particle $A^a(\theta)$ bounces back by keeping its original replica index a; (2) the second channel is described by the amplitude $Q(\theta)$ where the particle $A^a(\theta)$ changes its replica index $a \to b$ as result of the interaction (Fig. 3). Therefore we write

$$\mathcal{R}_{ab}(\theta) \ = \ P(\theta)\delta_{ab} + Q(\theta)(1-\delta_{ab}) \ . \tag{2.2}$$

In terms of the geometrical representation of Fig. 2, the dynamics consists in the free propagation of the particle on any one of the n sheets, according to its replica label: when the particle hits the boundary it can either remain on the same plane (with a probability $\mid P(\theta) \mid^2$) or redirect its motion to another of the $n-1$ planes (with a probability $\mid Q(\theta) \mid^2$).

The two amplitudes $P(\theta)$ and $Q(\theta)$ satisfy the unitarity conditions

$$\begin{aligned} &P(\theta)\, P(-\theta) + (n-1)\, Q(\theta)\, Q(-\theta) = 1 \ , \\ &P(\theta)\, Q(-\theta) + Q(\theta)\, P(-\theta) + (n-2)\, Q(\theta)\, Q(-\theta) = 0 \ , \end{aligned} \tag{2.3}$$

as well as the cross-unitarity equations

$$\begin{aligned} P\left(\tfrac{i\pi}{2} - \theta\right) &= -P\left(\tfrac{i\pi}{2} + \theta\right) \ , \\ Q\left(\tfrac{i\pi}{2} - \theta\right) &= \ Q\left(\tfrac{i\pi}{2} + \theta\right) \ . \end{aligned} \tag{2.4}$$

In the cross-unitarity equations we have chosen $S_{ab} = 1 - 2\delta_{ab}$ as the S–matrix relative to the collision processes of the replica in the bulk. The system of equations (2.3) and (2.4) admits two different classes of solutions depending whether $n \neq 2$ or $n = 2$.

For $n \neq 2$, the above crossing equations and the second of the unitarity equations may be identically satisfied by the following ansatz[5]

$$\begin{aligned} P(\theta) \;&=\; (n-2)\left(\frac{\theta}{i\pi} - \frac{1}{2}\right) f(\theta) \;\; ; \\ \\ Q(\theta) \;&=\; f(\theta) \;\; , \end{aligned} \tag{2.5}$$

with $f(\theta)$ being a crossing symmetric function

$$f(\theta) \;=\; f(i\pi - \theta) \;\; . \tag{2.6}$$

Plugging this ansatz into the first unitarity equation we obtain the additional equation

$$f(\theta)\, f(-\theta) \;=\; \frac{1}{4(n-2)^2} \frac{1}{\left(\frac{\theta}{2\pi}\right)^2 + \left(\frac{n}{4(n-2)}\right)^2} \tag{2.7}$$

for the function $f(\theta)$. The simplest "minimal" solution of (2.6) and (2.7) is given by[6]

$$f(\theta) = \frac{1}{(n-2)} \, \frac{1}{\left(\frac{\theta}{i\pi} - \frac{n}{2(n-2)}\right)} \, F(\theta) \;\; , \tag{2.8}$$

where

$$F(\theta) \;=\; \frac{\Gamma\left(\frac{n}{4(n-2)} + \frac{1}{2} - \frac{\theta}{2\pi i}\right) \Gamma\left(\frac{n}{4(n-2)} + \frac{\theta}{2\pi i}\right)}{\Gamma\left(\frac{n}{4(n-2)} + \frac{1}{2} + \frac{\theta}{2\pi i}\right) \Gamma\left(\frac{n}{4(n-2)} - \frac{\theta}{2\pi i}\right)} \;\; . \tag{2.9}$$

The function $F(\theta)$ admits the following integral representation

$$F(\theta) \;=\; \exp\left[i \int_0^\infty \frac{dt}{t} \frac{e^{-\frac{t}{2(n-2)}}}{\cosh\frac{t}{4}} \sin\frac{\theta t}{2\pi} \right] \;\; . \tag{2.10}$$

Note that the above minimal solution does not contain any free parameters. Apart from possible CDD factors, this seems to be a general property of the system of equations (2.3) and (2.4) for generic n. For $n = 2$, however, the situation is different. This is due to a simple reason: in fact, by unfolding two semi-infinite planes the system becomes in this case an ordinary Ising model (in the infinite plane) but with a line of defect. Hence

[5] A detailed discussion on the solution of eqs. (2.3) and (2.4) for $n \neq 2$ can be found in Appendix A.

[6] The most general solution is obtained by multiplying (2.8) by an arbitrary CDD factor, i.e. an arbitrary meromorphic function $\Phi(\theta)$ which satisfies both the equations $\Phi(\theta)\Phi(-\theta) = 1$ and $\Phi(\theta) = \Phi(i\pi - \theta)$.

for $n = 2$ the system of equations (2.3) and (2.4) admits extra solutions, more precisely those which belong to the one–parameter family of S-matrices of the Ising model with a line of defect which were determined in [20]. In the present notation they may be written as

$$P(\theta) = i\frac{\sin\chi\,\cosh\theta}{\sinh\theta - i\sin\chi}\ ;$$
$$Q(\theta) = \frac{\cos\chi\sinh\theta}{\sinh\theta - i\sin\chi}\ , \tag{2.11}$$

where

$$\sin\chi = -\frac{\Delta}{1+\frac{\Delta^2}{4}}\ . \tag{2.12}$$

These additional solutions at $n = 2$ may shed light on the identification of which physical situation the minimal solution (2.8) corresponds to. Let us compare, in fact, the minimal solutions $P(\theta)$ and $Q(\theta)$ in the limit $n \to 2$ with the reflection amplitudes of the defect line: in this limit $P(\theta)$ and $Q(\theta)$ go to 0 and to -1 respectively and therefore, from (2.11) and (2.12) we see that they correspond to an S-matrix of the defect line with an infinite value of the coupling constant Δ. This comparison suggests that the minimal solution (2.8), without any adjustable parameter, may correspond to n Ising models infinitely coupled at the boundary, i.e. to the strongly disordered case $\Delta \to \infty$.

Note that for $n = 1$ (and $\overline{h} = 0$) we cannot of course have any interaction between the replica and correspondingly the diagonal amplitude $P(\theta)$ in this case reduces to

$$P(\theta) = -i\coth\left(\frac{i\pi}{4} - \frac{\theta}{2}\right)\ , \tag{2.13}$$

which coincides with the reflection matrix of the pure Ising model with free boundary conditions. This result indicates that the simplest way to introduce the dependence on the (mean) magnetic field $\overline{h}$ is to multiply the minimal solution (2.8) by the CDD factor

$$H(\theta) \;=\; \tanh^2\left(\frac{\theta}{2} - \frac{i\pi}{4}\right)\frac{i\sinh\theta - \kappa}{i\sinh\theta + \kappa}\ . \tag{2.14}$$

For $n \to 0$ we have a well–defined limit and the exact boundary S-matrix is given in this case by

$$P(\theta) \;=\; \frac{\theta - \frac{i\pi}{2}}{\theta}\,\frac{\Gamma\left(\frac{1}{2} - \frac{\theta}{2\pi i}\right)\Gamma\left(\frac{\theta}{2\pi i}\right)}{\Gamma\left(\frac{1}{2} + \frac{\theta}{2\pi i}\right)\Gamma\left(-\frac{\theta}{2\pi i}\right)}\,H(\theta)\ ,$$
$$Q(\theta) \;=\; -\frac{i\pi}{2\theta}\,\frac{\Gamma\left(\frac{1}{2} - \frac{\theta}{2\pi i}\right)\Gamma\left(\frac{\theta}{2\pi i}\right)}{\Gamma\left(\frac{1}{2} + \frac{\theta}{2\pi i}\right)\Gamma\left(-\frac{\theta}{2\pi i}\right)}\,H(\theta)\ . \tag{2.15}$$

In the opposite limit $n \to \infty$, we find that $Q(\theta)$ goes to zero whereas $P(\theta)$ becomes

$$P(\theta) \;=\; -i \tanh^3 \left(\frac{i\pi}{4} - \frac{\theta}{2} \right) \frac{i \sinh\theta - \kappa}{i \sinh\theta + \kappa} \;, \tag{2.16}$$

i.e. a pure phase.

It is interesting to study the structure of the boundary bound states by varying n (in the following we will only consider the case $\overline{h} = 0$ since the discussion of the pole structure induced by the CDD term $H(\theta)$ may be found in [2]): from eqs. (2.8) and (2.9) we find that the positions of the poles are at:

$$\begin{aligned} \theta'_k &= (2k+1)\,\pi\, i + \frac{i\pi}{2} \left(\frac{n}{n-2} \right) \;\; ; \\ \theta''_l &= -2l\,\pi\, i - \frac{i\pi}{2} \left(\frac{n}{n-2} \right) \;\; , \end{aligned} \tag{2.17}$$

where $k, l = 0, 1, 2, ...$ For $n > 2$ there are no poles in the physical strip $0 \leq \mathrm{Im}\,\theta \leq \pi/2$. Vice-versa, for $n < 2$, as long as n belongs to the interval $\frac{4k+1}{2k+1} \leq n \leq \frac{8k+4}{4k+3}$ (respectively $\frac{8l}{4l+1} \leq n \leq \frac{4l+1}{2l+1}$), we find that in the physical strip there is the unique pole θ'_k (respectively θ''_l). These poles are associated to boundary bound states and their existence appears compatible with the analysis of the renormalization group relative to the variable Δ [15, 14]. In fact, for $n > 2$ Δ is a (marginal) relevant variable, hence of feeble effect at the short distance scales near the boundary; for $n < 2$, Δ becomes on the contrary a (marginal) irrelevant variable and therefore it may have quite a strong effect at the short distance scales near the boundary: this may result in an attractive force which can be strong enough to produce bound states. Note that the above poles (2.17) are generically simple poles but for specific values of n a pair of them may coincide, giving rise to a double order pole. The residue at the simple poles is related to the (square) of the boundary–particle couplings (Fig. 4) [2]

$$R_a^b(\theta) \;\sim\; \frac{i}{2} \frac{g_{a0\alpha} g_{\alpha b0}}{\theta - i v_{0a}^{\alpha}} \;\; . \tag{2.18}$$

So, for instance, looking at the pole at $\theta = -i\frac{\pi}{2}\left(\frac{n}{n-2}\right)$ with $0 < n < 1$, we have for the boundary–particle coupling in the diagonal channel $P(\theta)$

$$g_{i0\alpha}^2 = 2\sqrt{\pi} \frac{\Gamma\left(\frac{2n-3}{n-2}\right)}{\Gamma\left(\frac{3n-4}{2(n-2)}\right)} \;\; . \tag{2.19}$$

Analogous expressions are found for the residues at the other poles.

3 Quenched Correlation Functions

Quenched averaged correlation functions of the model may be computed by using the replica formalism and quantum field theory methods. Here the calculation for the first few is addressed, namely the one and two-point functions of the energy and magnetization operators. To this aim the following general formulas are needed

$$\begin{aligned}
&\overline{\langle\varphi(x)\rangle} = \lim_{n\to 0}\langle\varphi_a(x)\rangle \ ; \\
&\overline{\langle\varphi(x)\,\varphi(y)\rangle} = \lim_{n\to 0}\langle\varphi_a(x)\varphi_a(y)\rangle \ ; \\
&\overline{\langle\varphi(x)\rangle\,\langle\varphi(y)\rangle} = \lim_{n\to 0}\langle\varphi_a(x)\varphi_b(y)\rangle\mid_{a\neq b} \ .
\end{aligned} \tag{3.1}$$

In our case these formulas have to be further specified to take into account the boundary effects. Let us see how this can be done.

In the presence of boundary interactions, a convenient way to perform the calculation of the correlation functions is to employ a method based both on the boundary state wave function and the form factors relative to the local operators in the bulk[7]: assuming that the boundary is placed at the "time" $t = 0$ and described by its wave function $\mid B >$, the correlation functions may be in fact expressed as

$$\langle\mathcal{O}_1(x_1,t_1)\dots\mathcal{O}_p(x_p,t_p)\rangle = \frac{\langle 0\mid T_t\left[\mathcal{O}_1(x_1,t_1)\dots\mathcal{O}_p(x_p,t_p)\right]\mid B\rangle}{\langle 0\mid B\rangle} \ . \tag{3.2}$$

Since in this geometric setting the Hilbert space of the theory is the same as that in the bulk, the local operators $\mathcal{O}_a$ can be completely characterized by their bulk form factors

$$\langle A_{i_1}(\theta_1),\dots,A_{i_p}(\theta_p)\mid\mathcal{O}_a(0,0)\mid A_{i_{p+1}}(\theta_{p+1}),\dots,A_{i_q}(\theta_q)\rangle \ ,$$

irrespectively of the presence of the boundary. Hence, once the boundary state wave function is known, the calculation of the correlation functions (3.2) is in principle just a matter of introducing the completeness relationships of the intermediate states between the various operators. In our model the boundary state wave function is explicitly given by

$$\mid B\rangle = \exp\left[\frac{1}{2}\int_{-\infty}^{+\infty}d\theta K^{ab}(\theta)A_a(-\theta)A_b(\theta)\right]\mid 0\rangle \ , \tag{3.3}$$

where $K^{ab}(\theta)\equiv\hat{P}(\theta)\delta^{ab}+\hat{Q}(\theta)(1-\delta^{ab})$, with $\hat{P}(\theta)=P\left(\frac{i\pi}{2}-\theta\right)$ and $\hat{Q}(\theta)=Q\left(\frac{i\pi}{2}-\theta\right)$. With the above information, let us proceed to the calculation of some correlation functions.

[7]For the model under investigation in this paper, the form factors are all known, being the form factors of the thermal Ising model. Their expression may be found for instance in [19].

The simplest one is the averaged one–point function of the energy operator: in the language of the replica this is given by

$$\epsilon_0(t) \equiv \overline{\langle \epsilon(\rho) \rangle} \; = \; \lim_{n \to 0} \langle 0 \mid \epsilon_a(\rho) \mid B \rangle \; , \tag{3.4}$$

where $\rho \equiv (x,t)$ and t is the distance from the boundary. Once averaged, the one-point function $\overline{\langle \epsilon(t) \rangle}$ does not depend on x, as a consequence of the translation invariance along the boundary. In the bulk, the operator $\epsilon_a(x,t)$ couples only to the two–particle state with the same index a and its exact form factor is given by [19]

$$\begin{aligned} \langle 0 \mid \epsilon_a(x,t) \mid A_a(\theta_1) A_a(\theta_2) \rangle \; = \; & 2\pi m \, i \; \sinh \frac{\theta_1 - \theta_2}{2} \\ & \times \exp \left[-mt \left(\cosh \theta_1 + \cosh \theta_2 \right) + imx \left(\sinh \theta_1 + \sinh \theta_2 \right) \right] \; . \end{aligned} \tag{3.5}$$

Hence there is only one term of the boundary state wave function which contributes in this case (see Fig. 5) and we have

$$\overline{\langle \epsilon(t) \rangle} = \; -i \, m \int_0^\infty d\theta \sinh \theta \, \hat{P}(\theta) \, e^{-2mt \cosh \theta} \; . \tag{3.6}$$

In the above formula, $\hat{P}(\theta)$ is understood to be evaluated[8] at $n = 0$. Various profiles of this correlation function for different values of the mean magnetic field $\overline{h}$ may be found in Fig. 6. They present the typical cross–over associated to a relevant boundary operator: for $\overline{h} = 0$ the correlator present a short–distance singularity $\overline{\langle \epsilon(t) \rangle} \sim -1/(2t)$ whereas for $\overline{h} = \infty$ there is a swap of the overall sign $\overline{\langle \epsilon(t) \rangle} \sim 1/(2t)$. For finite values of $\overline{h}$ (however large), the corresponding curves follow the behavior of the curve at $\overline{h} = 0$ at very short distances while they tend to follow the behavior of the curve relative to $\overline{h} = \infty$ at large distances.

Let us consider now

$$\mathcal{G}(\rho_1, \rho_2) \; = \; \overline{\langle \epsilon(\rho_1) \, \epsilon(\rho_2) \rangle} \; = \; \lim_{n \to 0} \langle 0 \mid \epsilon_a(\rho_1) \epsilon_a(\rho_2) \mid B \rangle \; . \tag{3.7}$$

In terms of the replica, there are four possible graphs entering the above correlation functions (see Fig. 7) and correspondingly we have

$$\mathcal{G}(\rho_1, \rho_2) \; = \; I_1 + I_2 + I_3 + I_4 \; . \tag{3.8}$$

The first of them (Fig. 7.a) is just the product of the vacuum expectation values,

$$I_1 = \epsilon_0(t_1) \epsilon_0(t_2) \; . \tag{3.9}$$

[8]Unless explicitly stated, from now on both $\hat{P}(\theta)$ and $\hat{Q}(\theta)$ are meant to be the functions evaluated at $n = 0$.

Let us adopt in the following the notation $\overline{\tau} \equiv t_1 + t_2$, $\tau \equiv t_1 - t_2$, $x \equiv x_1 - x_2$, $r \equiv \sqrt{x^2 + \tau^2}$. The second term (see Fig. 7.b) is the bulk energy-energy correlation function, which, in terms of the Bessel function K_0 may be written as

$$I_2 \;=\; \left[\left(\frac{\partial}{\partial x} K_0(mr) \right)^2 + \left(\frac{\partial}{\partial \tau} K_0(mr) \right)^2 - m^2 \left(K_0(mr) \right)^2 \right] \;\; . \tag{3.10}$$

The remaining two terms relative to the graphs of Figs. 7c. and 7.d involve the amplitude $\hat{P}(\theta)$ and their expressions may be cast in the form

$$\begin{aligned} I_3 \;&=\; \left[2m \left(\frac{\partial}{\partial x} K_0(mr) \right) F(x,\overline{\tau}) - 2m K_0(mr) \left(\frac{\partial}{\partial x} F(x,\overline{\tau}) \right) \right] \;\; ; \\ I_4 \;&=\; \left[\left(mF(x,\overline{\tau}) \right)^2 - \left(\frac{\partial}{\partial x} F(x,\overline{\tau}) \right)^2 - \left(\frac{\partial}{\partial \overline{\tau}} F(x,\overline{\tau}) \right)^2 \right] \;\; , \end{aligned} \tag{3.11}$$

where we have introduced the auxiliary function

$$F(x,\tau) \;=\; \frac{1}{2} \int_{-\infty}^{+\infty} d\beta \, \hat{P}(\beta) \exp[-m\tau \cosh\beta + imx \sinh\beta] \;\; . \tag{3.12}$$

Altogether, the two-point function (3.7) can be finally expressed as

$$\begin{aligned} \mathcal{G}(\rho_1,\rho_2) \;&=\; \epsilon_0(t_1)\epsilon_0(t_2) + \left[\frac{\partial}{\partial x} K_0(mr) + mF(x,\overline{\tau}) \right]^2 + \left[\frac{\partial}{\partial \tau} K_0(mr) \right]^2 \\ &\quad - \left[\frac{\partial}{\partial \overline{\tau}} F(x,\overline{\tau}) \right]^2 - \left[mK_0(mr) + \frac{\partial}{\partial x} F(x,\overline{\tau}) \right]^2 \;\; . \end{aligned} \tag{3.13}$$

In the case of the energy operator, it is also interesting to calculate the following quenched averaged correlation function

$$\mathcal{G}_A(\rho_1,\rho_2) \;=\; \overline{\langle \epsilon(t_1) \rangle \langle \epsilon(t_2) \rangle} \;=\; \lim_{n \to 0} \langle \epsilon_a(x) \epsilon_b(x) \rangle \mid_{a \neq b} \;\; . \tag{3.14}$$

There are only two graphs which contribute to this correlation function. The first one is the disconnected term given by the product of the vacuum expectation values, eq. (3.9). The second one is the graph drawn in Fig. 8 which involves the off–diagonal amplitude $\hat{Q}(\theta)$. The correlator $\mathcal{G}_A(\rho_1,\rho_2)$ can be expressed in this case as

$$\begin{aligned} \mathcal{G}_A(\rho_1,\rho_2) \;&=\; \left[\left(\frac{\partial}{\partial x} Z(x,\overline{\tau}) \right)^2 + \left(\frac{\partial}{\partial \bar{\tau}} Z(x,\bar{\tau}) \right)^2 - \left(mZ(x,\bar{\tau}) \right)^2 \right] + \\ &\quad + \epsilon_0(t_1) \, \epsilon_0(t_2) \;\; , \end{aligned} \tag{3.15}$$

where we have defined the auxiliary function

$$Z(x,t) \;\equiv\; \frac{1}{2} \int_{-\infty}^{+\infty} d\beta \, \hat{Q}(\beta) \exp[-mt \cosh\beta + imx \sinh\beta] \;\; . \tag{3.16}$$

In the limit $\xi \to 0$ the composite operator $E_{ab}(\rho) = \lim_{\xi \to 0} \epsilon_a(\rho+\xi)\epsilon_b(\rho)$ does not present ultraviolet singularities: in fact, the two fields ϵ_a and ϵ_b do not have short–distance divergences in the bulk and they are linked to each other only through the boundary interaction. Therefore the above formula (3.15) can be specialized to the case $\rho_1 = \rho_2$ and studied correspondingly as one-point function of the field $E_{ab}(t)$: its profile versus the distance from the boundary is plotted in Fig. 9 for different values of the mean magnetic field. It is interesting to note the rapid crossover which occurs in this correlation function for large values of $\overline{h}$ at very short distance scales.

Let us now turn our attention to some correlation functions of the magnetization operators. The simplest is the one–point function of the disorder operator $\mu(\rho)$

$$\mu_0(t) \; = \; \overline{\langle \mu(\rho) \rangle} \; = \; \lim_{n \to 0} \langle 0 \mid \mu_a(\rho) \mid B \rangle \;\; . \tag{3.17}$$

In the high–temperature phase, the disorder operator $\mu_a(\rho)$ has a non-zero vacuum expectation value and couples to all states with an even number of particles with the same replica index: its explicit form factors are given by[9] [19]

$$\langle 0 \mid \mu_a(0,0) \mid A_a(\theta_1) \dots A_a(\theta_{2n}) \rangle \; = \; (-i)^n \prod_{i<j} \tanh \frac{\theta_i - \theta_j}{2} \;\; . \tag{3.18}$$

Since the boundary state consists of a condensate of Cooper pairs, i.e. couples of particles with equal and opposite momentum, we have to specialize the above formula to the case $\langle 0 \mid \mu_a(0) \mid A_a(-\theta_1)A_a(\theta_1) \dots A_a(-\theta_n)A_a(\theta_n) \rangle$. This matrix element can be conveniently written as

$$\langle 0 \mid \mu_a(0,0) \mid A_a(-\theta_1)A_a(\theta_1), \dots A_a(-\theta_n)A_a(\theta_n) \rangle \; = \; i^n \left(\prod_{i=1}^{n} \tanh \theta_i \right) \times \det \, W(\theta_i, \theta_j) \;\; , \tag{3.19}$$

where $W(\theta_i, \theta_j)$ is an $n \times n$ matrix whose elements are given by

$$W(\theta_i, \theta_j) \; = \; \left(\frac{2 \sqrt{\cosh \theta_i \cosh \theta_j}}{\cosh \theta_i + \cosh \theta_j} \right) \;\; . \tag{3.20}$$

The one–point function of the disorder operator is made of an infinite number of terms, as the one drawn in Fig. 10. Its final expression can be conveniently written as a Fredholm determinant

$$\begin{aligned} \overline{\langle \mu(t) \rangle} \;\; &= \;\; \sum_{n=0}^{\infty} \frac{1}{n!} \int_{-\infty}^{\infty} d\theta_1 \dots d\theta_n \, z^n \left(\prod_{k=0}^{n} i \, \tanh \theta_k \, \hat{P}(\theta_k) \, e^{-2mt \cosh \theta_k} \right) \det \, W(\theta_i, \theta_j) \; = \\ &= \; \det \left(1 + z \, \mathcal{W} \right) \;\; , \end{aligned} \tag{3.21}$$

[9] The magnetization field defined by the Form Factors normalized as in eq. (3.18) differs from the corresponding conformal field only by a normalization constant, $\mu(\rho) = \mathcal{F} \, \mu_{conf}(\rho)$, where $\mathcal{F} = 2^{-1/12} e^{1/8} A^{-3/2} m^{-1/8}$ and $A = 1.282427$ (Glasher constant).

where the kernel of the integral operator is given by

$$\mathcal{W}(\theta_i, \theta_j) \;=\; \frac{E(\theta_i, mt)E(\theta_j, mt)}{\cosh\theta_i + \cosh\theta_j} \;, \tag{3.22}$$

and

$$E(\theta, mt) \;=\; e^{-mt\cosh\theta}\,\left(i\hat{P}(\theta)\,\tanh\theta\right)^{1/2} \quad , \quad z \;=\; \frac{1}{2\pi} \;. \tag{3.23}$$

As consequence of the translation invariance along the boundary, $\mu_0(t)$ depends only on its distance t from the boundary. In terms of the eigenvalues of the integral operator and their multiplicity, $\overline{\mu(t)}$ can be also expressed as

$$\overline{\mu(t)} \;=\; \prod_{i=1}^{\infty} (1 + z\,\lambda_i)^{a_i} \quad . \tag{3.24}$$

As far as mt is finite, the kernel is square integrable and therefore its properties are those of a bounded symmetric integral operator [21]. For large values of mt, $\overline{\langle\mu(t)\rangle}$ falls off exponentially to its bulk vacuum expectation value. However, when $mt \to 0$, the integral operator becomes unbounded: in this case, the multiplicity of the eigenvalues grows logarithmically as $a(t) \sim \frac{1}{\pi}\ln\left(\frac{1}{mt}\right)$ and the one-point function presents a power law behavior $\overline{\langle\mu(t)\rangle} \sim A/(2t)^{\zeta}$. To determine ζ, observe that as long as $n \neq 2$ (which we always assume to be the case in the following) and $\overline{h} \neq \infty$, we have $\lim_{\theta\to\infty}\hat{P}(\theta) = -i$. Let us denote this limit as $\hat{P}_-$. For $n \neq 2$ and $\overline{h} = \infty$, we have $\lim_{\theta\to\infty}\hat{P}(\theta) = i$, instead. This limit value will be denoted by $\hat{P}_+$. To study the short distance behavior $mt \to 0$, we can reasonably substitute $\hat{P}(\theta)$ with its asymptotic limits $\hat{P}_\pm$. The eigenvalues of the integral operator then become dense in the interval $(0, \infty)$ according to the distribution

$$\lambda(p) \;=\; \frac{2\pi}{\cosh\pi p}$$

and for the exponent $\zeta_\pm$ relative to the two cases we find

$$\zeta_\pm \;= -\frac{1}{\pi}\int_0^\infty dp\,\ln\left(1 \pm \frac{2\pi z}{\cosh p}\right) \;=\; -\frac{1}{8} + \frac{1}{2\pi^2}\arccos^2(\mp 1) = \begin{cases} \frac{3}{8} \\ -\frac{1}{8} \end{cases} \tag{3.25}$$

The profile of this one-point function is drawn in Fig. 11 for several values of $\overline{h}$: the observed cross-over behavior of the curves by varying $\overline{h}$ is perfectly analogous to the one of the energy operator.

Let us conclude this section with the discussion relative to the (averaged) two-point function of the magnetization operator $\sigma(\rho)$. In the bulk, this operator has non–vanishing matrix elements on an odd number of particles and their expression is given by the same formula as (3.18) [19]. Consider first

$$\mathcal{G}^\sigma(\rho_1, \rho_2) \;=\; \overline{\langle\sigma(\rho_1)\sigma(\rho_2)\rangle} = \lim_{n\to 0}\langle 0 \mid \sigma_a(\rho_1)\sigma_a(\rho_2) \mid B\rangle \;. \tag{3.26}$$

There are two kinds of graphs entering the above correlator (see Fig. 12). The first does not involve the boundary and therefore the sum of such graphs gives rise to the known correlation function in the bulk which is expressible in terms of Painleve' function [22]. The second set of graphs is made of an arbitrary number of pairs of particles A_a emitted by the boundary and absorbed by the two operators. The two operators, in turn, are also linked together by an arbitrary (odd) number of intermediate particle states. The first non-trivial contribution to this correlation function is the one shown in Fig. 13, given by

$$J(\rho_1, \rho_2) \; = \; 2g^2 F(x, \bar{\tau}) \; , \tag{3.27}$$

where g denotes the (constant) one-particle form factor of the magnetization operator $\langle 0 \mid \sigma(0)_a \mid A_b(\beta) \rangle = g\delta_{ab}$ and the function $F(x,t)$ is defined in (3.12). A convenient form of the series resulting from the graphs of Fig. 12 is presently unknown.

Let us consider now the other type of two–point averaged correlation function

$$\mathcal{G}^{\sigma}_{A}(\rho_1, \rho_2) \; = \; \overline{\langle \sigma(\rho_1) \rangle \, \langle \sigma(\rho_2) \rangle} = \lim_{n \to 0} \langle \sigma_a(\rho_1) \sigma_b(\rho_2) \rangle \mid_{a \neq b} \quad . \tag{3.28}$$

The graphs contributing to this correlation function are those shown in Fig. 14. This time the boundary can emit an arbitrary number of pairs of particles of type $A_a A_a$, $A_b A_b$ or $A_a A_b$: the former two pairs are individually absorbed by each operator whereas the latter link the operators to each other. The simplest (non–disconnected) term of the resulting series is given in this case by

$$J^{(1)}_{A}(\rho_1, \rho_2) \; = \; 2g^2 Z(x, \bar{t}) \; , \tag{3.29}$$

where the function $Z(x, \bar{t})$ is defined in eq. (3.16). The above discussion can be easily generalized to the correlator $\mathcal{G}^{\mu}_{A}(\rho_1, \rho_2) = \overline{\langle \mu(\rho_1) \rangle \langle \mu(\rho_2) \rangle}$ as well. In this case the lowest contribution of the series originates from a graph like the one of Fig. 8 and its explicit expression is given by

$$\begin{aligned} J^{(2)}_{A}(\rho_1, \rho_2) \; = \; \int_0^{+\infty} \frac{d\beta_1}{2\pi} \int_{-\infty}^{+\infty} \frac{d\beta_2}{2\pi} \, \tanh^2(\frac{\beta_1 - \beta_2}{2}) \, \hat{Q}(\beta_1) \, \hat{Q}(\beta_2) \, \times \\ e^{-m(t_1+t_2)(\cosh\beta_1 + \cosh\beta_2)} \cos[m(x_1 - x_2)(\sinh\beta_1 + \sinh\beta_2)] \; . \end{aligned} \tag{3.30}$$

It can be rewritten as

$$J^{(2)}_{A}(\rho_1, \rho_2) \; = \; 4 \sum_{l=0}^{+\infty} \Big[(2l+1) \, \Big(\mathcal{Z}_{2l+2}(x, \bar{\tau}) \mathcal{Z}_{2l}(x, \bar{\tau}) - \mathcal{Z}^2_{2l+1}(x, \bar{\tau}) \Big) + \tag{3.31}$$

$$+ (2l+2) \, \Big(\mathcal{Z}_{2l+3}(x, \bar{\tau}) \mathcal{Z}_{2l+1}(x, \bar{\tau}) - \mathcal{Z}^2_{2l+2}(x, \bar{\tau}) \Big) \Big] \; , \tag{3.32}$$

where

$$\mathcal{Z}_l(x,t) \; \equiv \; \frac{1}{2} \int_{-\infty}^{+\infty} \frac{d\beta}{2\pi} \left(\tanh\frac{\beta}{2} \right)^l \, \hat{Q}(\beta) \exp[-mt\cosh\beta + imx\sinh\beta] \, . \tag{3.33}$$

Since the rate of convergence of the functions $\mathcal{Z}_l(x,t)$ becomes faster and faster by increasing l, the series (3.31) can be efficiently estimate by means of the first few terms.

As was the case for the energy operator, we can define the operators

$$\Sigma_{ab}(\rho) = \lim_{\xi\to 0} \sigma_a(\rho+\xi)\sigma_b(\rho) \;\; ; \;\; \Upsilon_{ab}(\rho) = \lim_{\xi\to 0} \mu_a(\rho+\xi)\mu_b(\rho) \;\; , \tag{3.34}$$

without facing any short–distance singularities. It is therefore possible to study the correlator $\mathcal{G}_A^{\sigma,\mu}(\rho_1,\rho_2)$ in the limit $\rho_1 \to \rho_2$, the so-called Edwards-Anderson (EA) order parameters $\overline{\langle\sigma(\rho)\rangle^2}$ and $\overline{\langle\mu(\rho)\rangle^2}$. The profile of the Edwards-Anderson order parameter $\overline{\langle\mu(\rho)\rangle^2}$ for different values of $\bar{h}$ by using the lowest order approximation (3.30) is drawn in Fig. 15. Presently however it is quite difficult to make any comparison with the lowest order expression in Δ ($\bar{h}=0$) for such parameter

$$\overline{\langle\mu(t)\rangle^2} \sim \Delta \frac{1}{r^{1/4}} \;\; , \tag{3.35}$$

which was obtained by Cardy [15]. This difficulty is due to several reasons: (a) the different methods which were employed in the two cases (Cardy obtained in fact (3.35) by using boundary conformal perturbation theory; on the other hand, our approach is based on the scattering theory relative to the off–critical excitations); (b) the lack of an exact re-summation of the series originated from the graphs of Fig. 14 which, if known, would permit in principle a comparison between the two methods above and finally (c) that the result (3.35) applies for small values of Δ whereas our scattering theory seems to apply to the opposite limit $\Delta \to \infty$ instead.

4 Boundary Thermodynamical Bethe Ansatz

Once the exact S–matrix of a model is known, finite–size effects and associated thermodynamical quantities can be calculated by means of the Thermodynamical Bethe Ansatz (TBA): the case of systems with relativistic invariance and a cylinder geometry with periodic boundary conditions has been put forward in [12]. What is of interest for us here is the generalization of the TBA to systems with boundary: such generalization can be found discussed in [11].

Consider then an Ising model defined on a cylinder of width L and length R with boundary conditions at its extremities described by the reflection scattering theory of Sect. 2 (see Fig. 16.a). Choosing as direction of the time the horizontal axis between the two boundaries, the partition function of the model can be expressed as

$$Z = \langle B \mid \exp(-RH) \mid B \rangle \;\; , \tag{4.1}$$

where H is the Hamiltonian of the bulk system with periodic boundary conditions. In the limit $mR \gg 1$, the partition function reduces to

$$Z \sim g_I g_{II}\, e^{-RE_0} \ , \tag{4.2}$$

where E_0 is the ground–state energy of the system whereas g_I and g_{II} are the boundary degeneracy at each end of the cylinder. The R–independent term

$$\mathcal{S}_{I,II} \ = \ \ln g_{I,II} \tag{4.3}$$

can be then interpreted as boundary entropies of the system [13]. They can be computed by using the boundary Thermodynamical Bethe Ansatz [11]. The application of this method requires first of all to look at cylinder geometry of Fig. 16.a in a different way, namely the time evolution should be regarded as it takes place along the vertical axes, i.e. along the circumference of length L. Hence, the dynamics consists in a set of N particles which move and scatter each other along the segment of length R until they reach the boundaries: then, they are reflected off with amplitudes $\mathcal{R}_{ab}(\theta)$. The finite geometry of the system induces a quantization condition on the momenta of the particles which can be obtained as follows. Let n_a be the number of particles of replica index a, with $\sum_a n_a = N$. Consider now one of N particles, of species b and send it on a "round trip" along the cylinder (Fig. 16.b): after coming back to the same location, the wave function of the N particles has picked up a new phase shift. In fact, each time that the particle scatters off a like particle it picks up a -1 from their bulk S-matrix (all other scattering processes in the bulk with particles of different species do not contribute since the S–matrix in these cases is simply $+1$); in addition to these processes, there is an additional phase $R_{bk}(\theta)R_{kb}(\theta)$ (sum on the internal index k) due to the scattering off the two boundaries. Since the total wave function of the N particle state is assumed to be periodic under this "round trip" along the cylinder, we get the quantization condition

$$e^{2iRm_b \sinh(\theta)}(-1)^{n_b+n_k-1}(\Lambda_a(\theta))^2 = 1 \ , \tag{4.4}$$

where $\Lambda_a(\theta)$, $a = 1, 2, \ldots, n$, are eigenvalues of the reflection matrix $\mathcal{R}_{bk}(\theta)$. They can be found explicitly since any $n \times n$ matrix of the form

$$M_{ij} = (P - Q)\delta_{ij} + Q$$

has only two types of eigenvalues: $\lambda_1 = P+(n-1)Q$ with multiplicity one and $\lambda_2 = P-Q$, which is $(n-1)$ degenerate.

With this information, the analysis that follows is quite standard (see for instance [11]) and therefore we only sketch the main steps here. Eq. (4.4) puts a constraints among the physical rapidities and therefore for each particle in the interval θ and $\theta + d\theta$

we can define the density of holes, $\rho_i^h(\theta)$, and of actually occupied states, $\rho_i(\theta)$. Hence, the density of available states for particles of species a is $\rho_a(\theta) + \rho_a^h(\theta)$ which is given by

$$2\pi(\rho_a(\theta) + \rho_a^h(\theta)) = m_a \cosh(\theta) + \frac{1}{2R}\Phi_a(\theta) \ , \tag{4.5}$$

where we have introduced

$$\Phi_a(\theta) = -2i\frac{d}{d\theta}\ln \Lambda_a(\theta) - 2\pi\delta(\theta) \ . \tag{4.6}$$

The delta function term is introduced in order to remove the unwanted solution $\theta = 0$. The partition function is obtained by expressing the Helmholtz's free energy as a functional of the density of states (holes and particles) and minimize it. The final expression of the boundary entropy is given by the massless limit of

$$\mathcal{S}_b = \lim_{m\to 0} \sum_{i=1}^{n} \int \frac{d\theta}{4\pi} \Phi_i(\theta) \ln(1 + e^{-\epsilon_i(\theta)}) \ , \tag{4.7}$$

where $\mathcal{S}_b$ is the boundary entropy at one end and the pseudo–energies $\epsilon_i(\theta)$ are given by the simple expression

$$\epsilon_i(\theta) = m_i R \cosh(\theta) \ . \tag{4.8}$$

since the bulk S-matrix is ± 1.

The formula (4.7) becomes then

$$\mathcal{S}_b = \frac{n}{\pi} \int_0^\infty dx \frac{1}{1+x^2} \ln(1 + e^{-2\pi a x}) \ , \tag{4.9}$$

where $mR\cosh(\theta) \equiv 2\pi a x$ and $a = \overline{h}^2 R/(4\pi)$. Note that each species gives exactly the same contribution and so we have an overall factor of n in our expression. The above integral can be computed exactly

$$\mathcal{S}_b = n \ln \left(\frac{\sqrt{2\pi}}{\Gamma(a + \frac{1}{2})} \left(\frac{a}{e} \right)^a \right) \ . \tag{4.10}$$

For $n = 1$ (which corresponds to the pure Ising model) we obtain the correct boundary entropy difference $\Delta\mathcal{S}_b = \ln\sqrt{2}$ (for $a = \infty$ and $a = 0$) [13]. The entropy difference of the disordered model ($n = 0$) is computed by taking the derivative of the ground state degeneracy with respect to n and let $n \to 0$. This gives $\Delta\mathcal{S}_b = \ln\sqrt{2}$, exactly the same result as in the pure Ising model.

5 Conclusions

In this paper we have proposed an exact scattering theory in the replica space of n species of particles A_a (in the limit $n \to 0$) to describe the dynamics of the two–dimensional Ising

model coupled to a boundary random magnetic field. By using methods borrowed from boundary quantum field theories, we have then computed averaged correlation functions of the order parameters as well as finite–size effects of the system defined on a strip. It would be obviously interesting to test the feasibility of this approach for analyzing other models with random interactions localized on the boundary.

Acknowledgments. We wish to thank J. Cardy, S. Franz, S. Guruswamy and R. Monasson for useful conversations and comments. We are extremely grateful to J.M. Maillard for helpful discussions. One of us (GM) would like to thank the organizers of the workshops at the H. Poincare' Institute in Paris and the Institute of Theoretical Physics in Santa Barbara for the warm hospitality during the staying at these institutes, where part of this work has been done. (MM) would like to thank S. Randjbar–Daemi and the High–Energy group at ICTP for the warm hospitality.

Note Added. We become aware of the reference [14] after finishing the present work. We thank L. Turban for his observation.

Related work, on the 2-dimensional Dirac theory in semi-infinite space with random boundary interactions, has recently been done independently by S. Guruswamy and A.W.W. Ludwig [23].

Appendix A

In this appendix we briefly discuss the most general solution of the boundary unitarity and cross-unitarity equations (2.3) and (2.4) for $n \neq 2$. Let's initially define a function $D(\theta) = P(\theta) - Q(\theta)$. It's easy to see that the unitarity equations impose

$$D(\theta)D(-\theta) \,=\, 1 \ . \tag{A.1}$$

Therefore, substituting $P(\theta) = D(\theta) + Q(\theta)$ into the first unitarity equation (2.3), we find

$$D(\theta)Q(-\theta) + D(-\theta)Q(\theta) + nQ(\theta)Q(-\theta) = 0 \ . \tag{A.2}$$

Dividing by $Q(\theta)Q(-\theta)$, we have

$$\frac{D(\theta)}{Q(\theta)} + \frac{D(-\theta)}{Q(-\theta)} + n = 0 \ . \tag{A.3}$$

Define $T(\theta)$ by

$$T(\theta) = \frac{D(\theta)}{Q(\theta)} + \frac{n}{2} \ . \tag{A.4}$$

From (A.3) we see that $T(\theta)$ is an odd function. Cross-unitarity requires

$$T(i\pi - \theta) + T(\theta) = n - 2 \ . \tag{A.5}$$

With the position $D(\theta) = d(\theta)(2T(\theta) - n)$, we see that $d(\theta)$ has to satisfy

$$d(\theta)d(-\theta) = \frac{1}{(2T(\theta) - n)(2T(-\theta) - n)} \ . \tag{A.6}$$

From this point on the analysis is standard and one can easily find two solutions for $d(\theta)$ (up to CDD factors)

$$d(\theta) \,=\, \frac{1}{(2T(\theta) - n)} \frac{\Gamma(1 - \frac{n-2T(\theta)}{4(n-2)})\Gamma(\frac{1}{2} - \frac{n+2T(\theta)}{4(n-2)})}{\Gamma(1 - \frac{n+2T(\theta)}{4(n-2)})\Gamma(\frac{1}{2} - \frac{n-2T(\theta)}{4(n-2)})} \ . \tag{A.7}$$

$$d(\theta) \,=\, \frac{-1}{(2T(\theta) + n)} \frac{\Gamma(1 + \frac{n+2T(\theta)}{4(n-2)})\Gamma(\frac{1}{2} + \frac{n-2T(\theta)}{4(n-2)})}{\Gamma(1 + \frac{n-2T(\theta)}{4(n-2)})\Gamma(\frac{1}{2} + \frac{n+2T(\theta)}{4(n-2)})} \ . \tag{A.8}$$

These are general expressions that solve unitarity and cross-unitarity conditions provided $T(\theta)$ is an odd function satisfying the equation (A.5). The simplest solution for $T(\theta)$ which gives the correct analytic behavior is

$$T(\theta) = (n-2)\frac{\theta}{i\pi} \ . \tag{A.9}$$

With this choice of $T(\theta)$, the two solutions equations (A.7) and (A.8) are easily seen to be connected by a CDD factor. They differ in the positions of the poles: the first one has poles in the physical strip for $n > 2$, the second one, instead, for $n < 2$. This last feature is one of the reasons to use the latter solution for the physical scattering amplitudes in the replica space.

References

[1] J.L. Cardy, *Nucl. Phys.* **B 240** [FS 12] (1984), 514; *Nucl. Phys.* **B 270** (1986), 186; *Nucl. Phys.* **B 324** (1989), 581.

[2] S. Ghoshal and A. Zamolodchikov, *Int. J. Mod. Phys.* **A 9** (1994), 3841.

[3] A. Fring and R. Köberle, *Nucl. Phys.* **B 421** (1994), 159; *Nucl. Phys.* **B 419** (1994), 647; *Int. J. Mod. Phys.* **A 10** (1995), 739.

[4] K. Binder, in *Phase transitions and critical phenomena*, vol.8, (1983), Academic Press (London).

[5] H.W. Diehl, in *Phase transitions and critical phenomena*, vol.10, (1986), Academic Press (London).

[6] I. Affleck and A. Ludwig, *Nucl. Phys.* **B 352**, (1991), 849; I. Affleck and A. Ludwig, *Phys. Rev. Lett.* **67** (1991), 161; P. Fendley, *Phys. Rev. Lett.* **71** (1993), 2485.

[7] P. Fendley, A. Ludwig and H. Saleur, *Phys. Rev.* **B 52** (1995), 8934.

[8] F. Lesage, H. Saleur and S. Skorik, *Nucl. Phys.* **B 474** (1996), 602.

[9] R. Konik, A. LeClair and G. Mussardo, *Int. J. Mod. Phys.* **A 11** (1996), 2765.

[10] R. Chatterjee and A. Zamolodchikov, *Mod. Phys. Lett.* **A 9** (1994), 2227; R. Chatterjee, *Nucl. Phys.* **B 468** (1996), 439.

[11] A. LeClair, G. Mussardo, H. Saleur and S. Skorik, *Nucl. Phys.* **B 453** (1995), 581.

[12] Al.B. Zamolodchikov, *Nucl. Phys.* **B 342** (1990), 695.

[13] I. Affleck and A. Ludwig, *Phys. Rev. Lett.* **87** (1991), 161.

[14] F. Igloi, L. Turban and B. Berche, *J. Phys. A: Math. Gen.* **24** (1991), L1031.

[15] J.L. Cardy, *J. Phys. A: Math. Gen.* **24** (1991), L1315.

[16] A.B. Zamolodchikov, Al.B. Zamolodchikov, *Ann. Phys.* **120** (1979), 253.

[17] G. Mussardo, *Phys. Rep.* **218** (1992), 215, and references therein.

[18] R. Köberle and J.A. Swieca, *Phys. Lett.* **B 86** (1979), 209; M. Sato, T. Miwa and M. Jimbo, *Proc. Japan Acad.* **A 53** (1977), 147.

[19] B. Berg, M. Karowski and P. Weisz, *Phys. Rev.* **D 19** (1979), 2477; V.P. Yurov and Al.B. Zamolodchikov, *Int. J. Mod. Phys.***A 6** (1991), 3419; J.L. Cardy and G. Mussardo, *Nucl. Phys.***B 340** (1990), 387; O. Babelon and D. Bernard, *Phys. Lett.* **B 288** (1992), 113.

[20] G. Delfino, G. Mussardo and P. Simonetti, *Nucl. Phys.* **B 432** [FS] (1994), 518.

[21] M. Bocher, *An Introduction to the Study of Integral Equations*, Hafner Publishing Co. N.Y.

[22] T.T. Wu, B.M. McCoy, C.A. Tracy and E. Barouch, *Phys. Rev.* **B 13** (1978), 316; B.M. McCoy, C.A. Tracy and T.T. Wu, *Jour. Math. Phys.* **18** (1977), 1058.

[23] S. Guruswamy and A.W.W. Ludwig, in preparation.

Figure Caption

Figure 1 . Graphs of the perturbative series: (a) pure system (b) system with disorder.

Figure 2 . Replica space.

Figure 3 . Reflection amplitudes in replica space.

Figure 4 . Boundary bound state and boundary–particle couplings.

Figure 5 . Graph of the averaged one–point function of the energy operator.

Figure 6 . Profiles of the one–point function of the energy operator versus its distance from the boundary for different values of κ: $\kappa = 1$ (long dashes), $\kappa = -1$ (short dashes) and $\kappa = -10$ (full line).

Figure 7 . All possible graphs of the averaged two–point function of the energy operator.

Figure 8 . Diagram relative to $\overline{\langle \epsilon(\rho_1)\, \epsilon(\rho_2)\rangle}$.

Figure 9 . Profiles of the one–point function $\overline{\langle \epsilon(t)\rangle^2}$ for different values of κ: $\kappa = 1$ (long dashes), $\kappa = -1$ (short dashes) and $\kappa = -10$ (full line).

Figure 10 . One of the diagrams entering the one–point function of the disorder operator.

Figure 11 . Profiles of the one–point function $\overline{\langle \mu(t)\rangle}$ at the lowest order approximation for different values of κ: $\kappa = 1$ (long dashes), $\kappa = -1$ (short dashes) and $\kappa = -10$ (full line).

Figure 12 . Diagrams entering the averaged two–point function of the magnetization operator.

Figure 13 . Simplest graph contributing to the averaged two–point function of the magnetization operator.

Figure 14 . Diagrams contributing to the two–point function $\overline{\langle \mu(\rho_1)\rangle\, \langle\, \mu(\rho_2)\rangle}$.

Figure 15 . Profiles of the EA parameter $\overline{\langle \mu(t)\rangle^2}$ at the lowest order approximation for different values of κ: $\kappa = 1$ (long dashes), $\kappa = -1$ (short dashes) and $\kappa = -10$ (full line).

Figure 16 . Strip geometry (a) and "round trip" (b) of the TBA quantization equation.

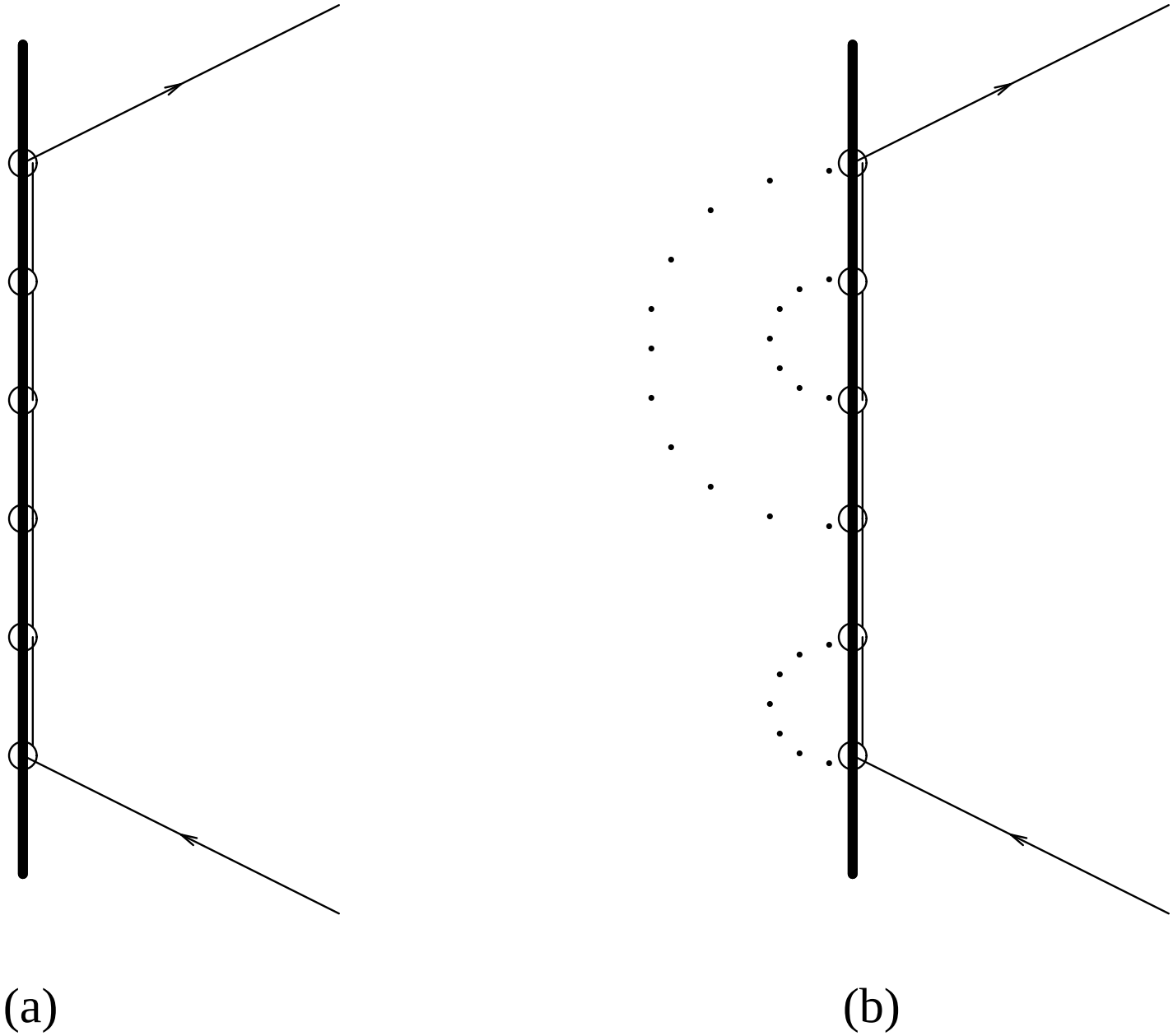

Figure 1

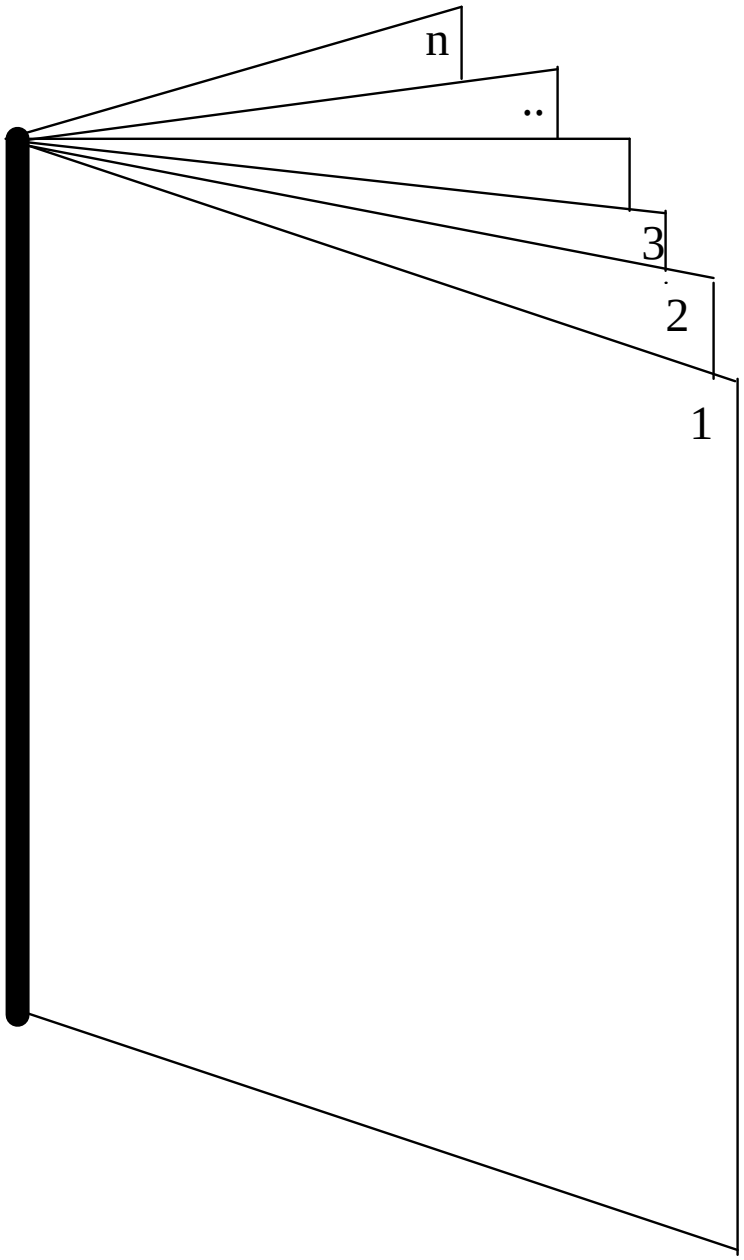

Figure 2

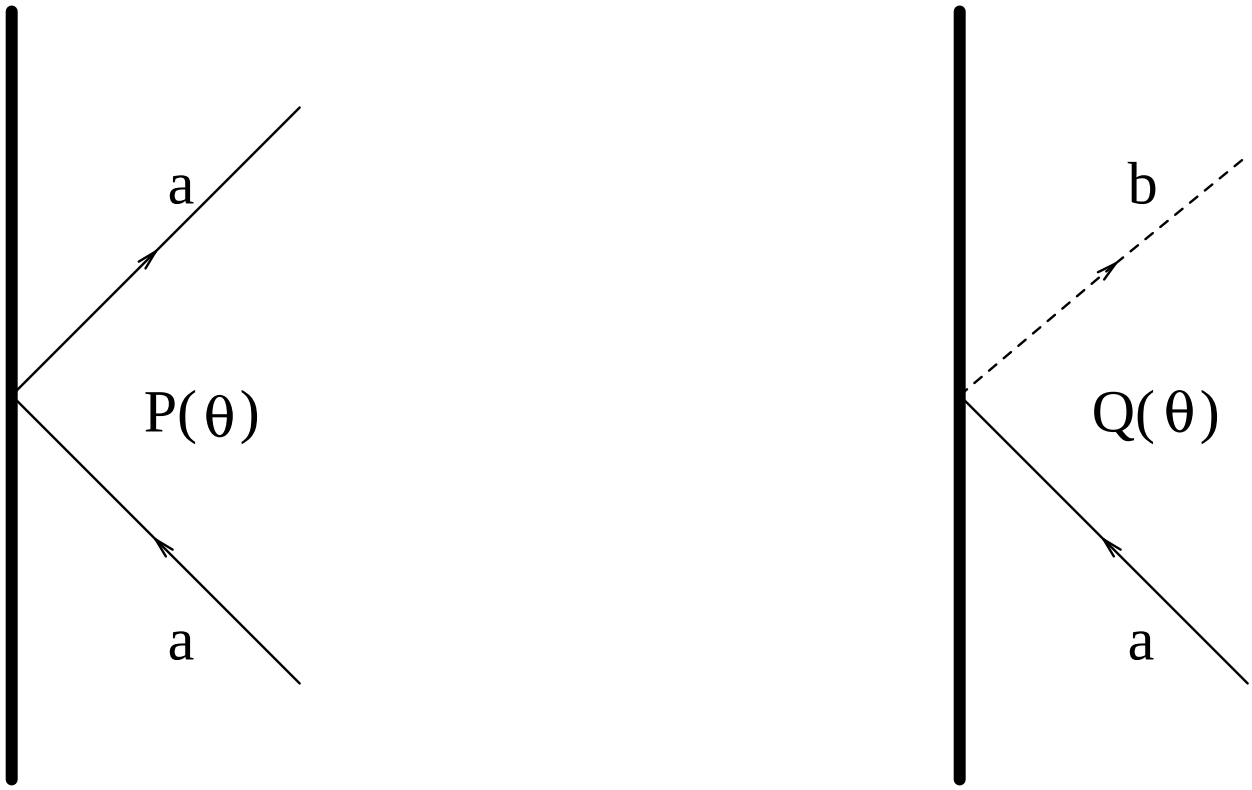

Figure 3

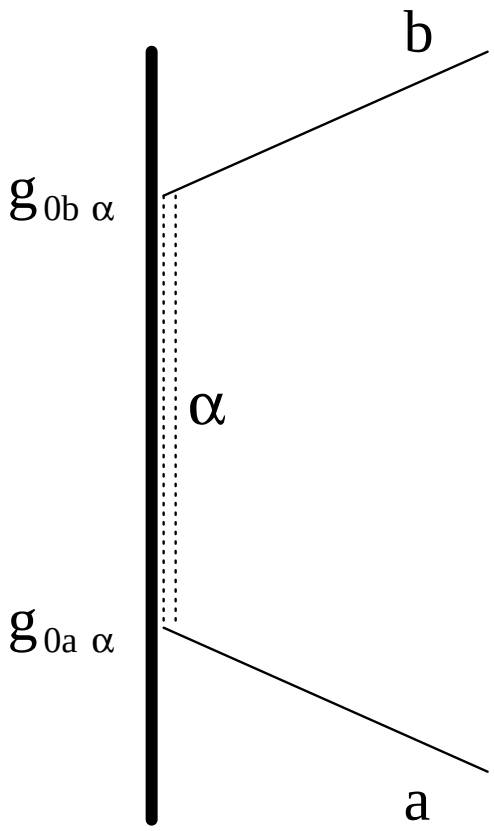

Figure 4

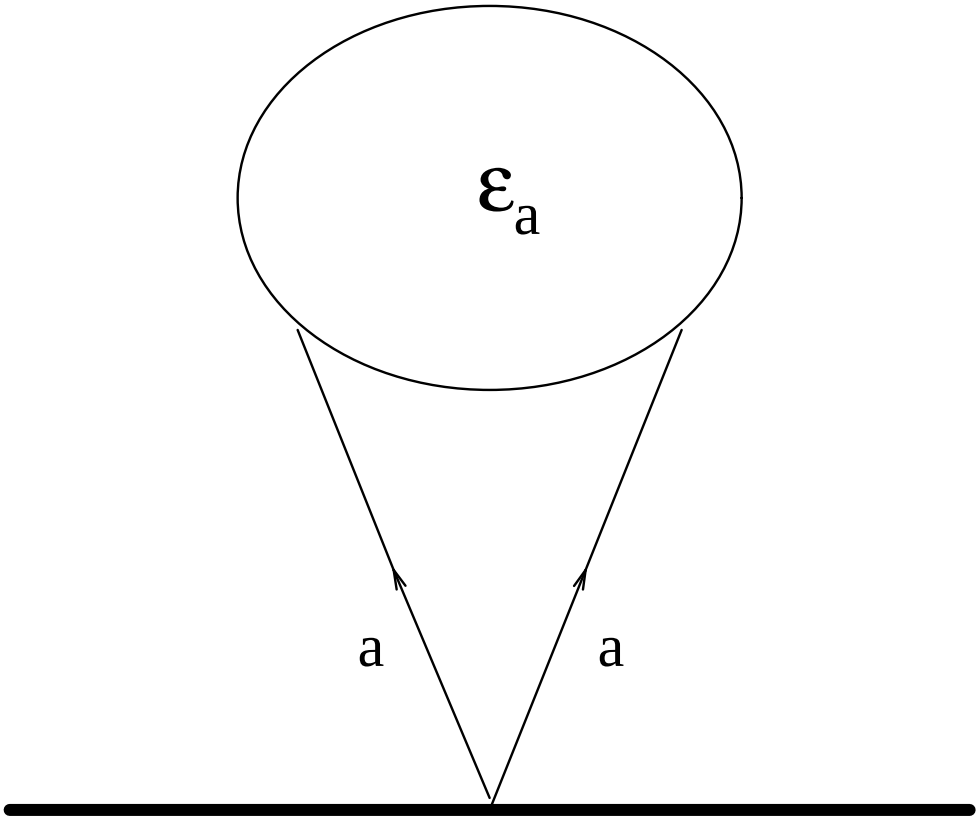

Figure 5

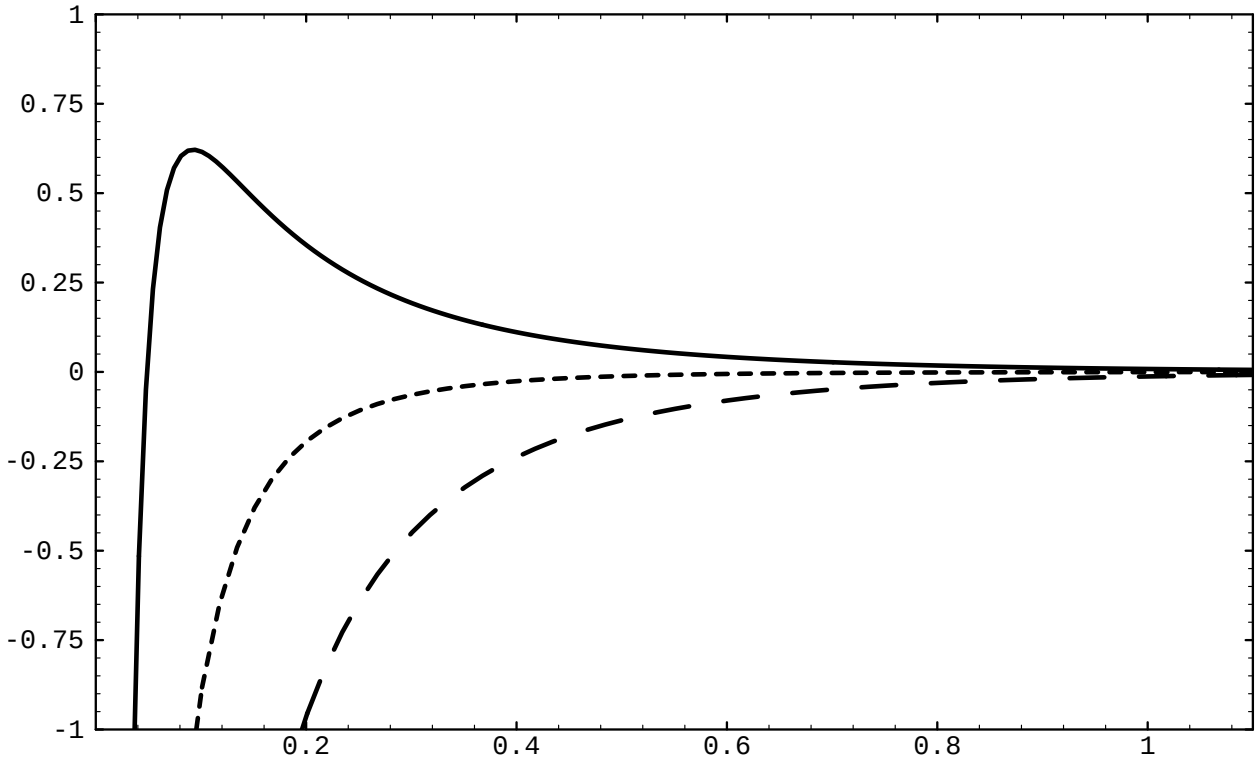

Figure 6

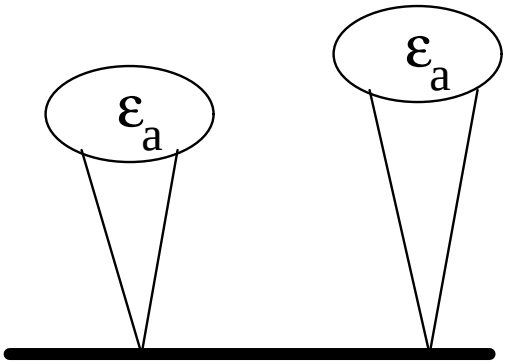

(a)

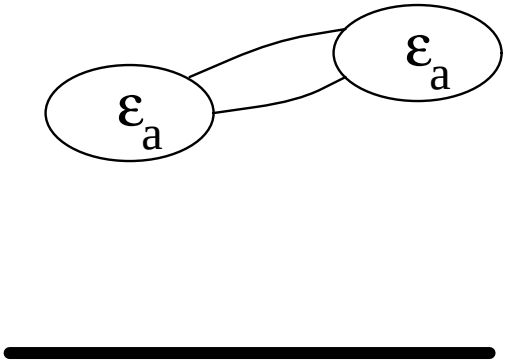

(b)

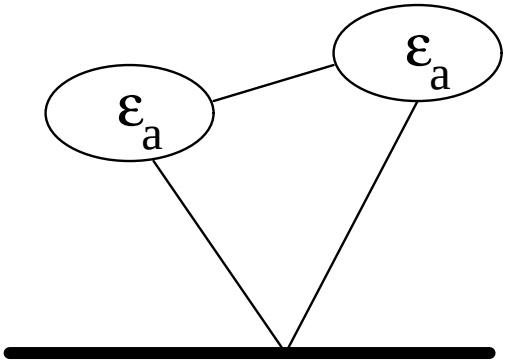

(c)

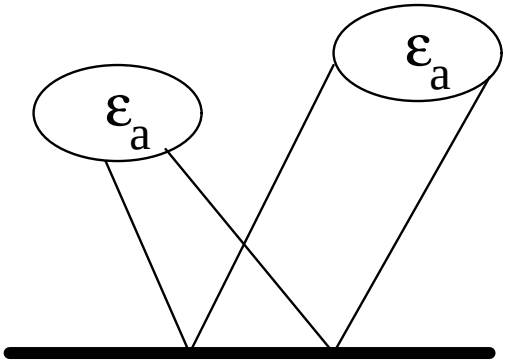

(d)

Figure 7

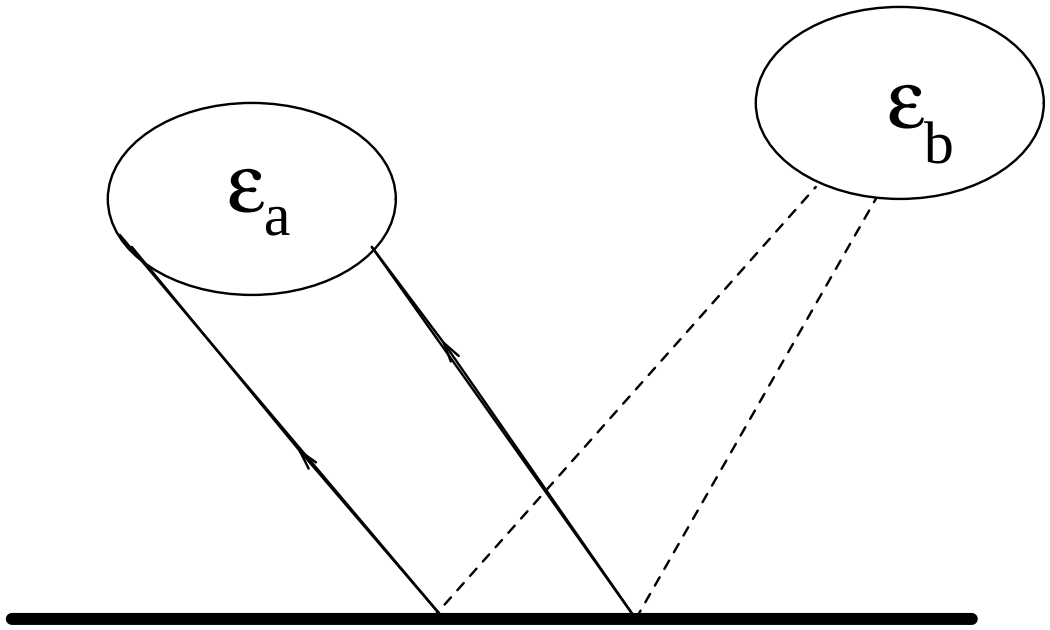

Figure 8

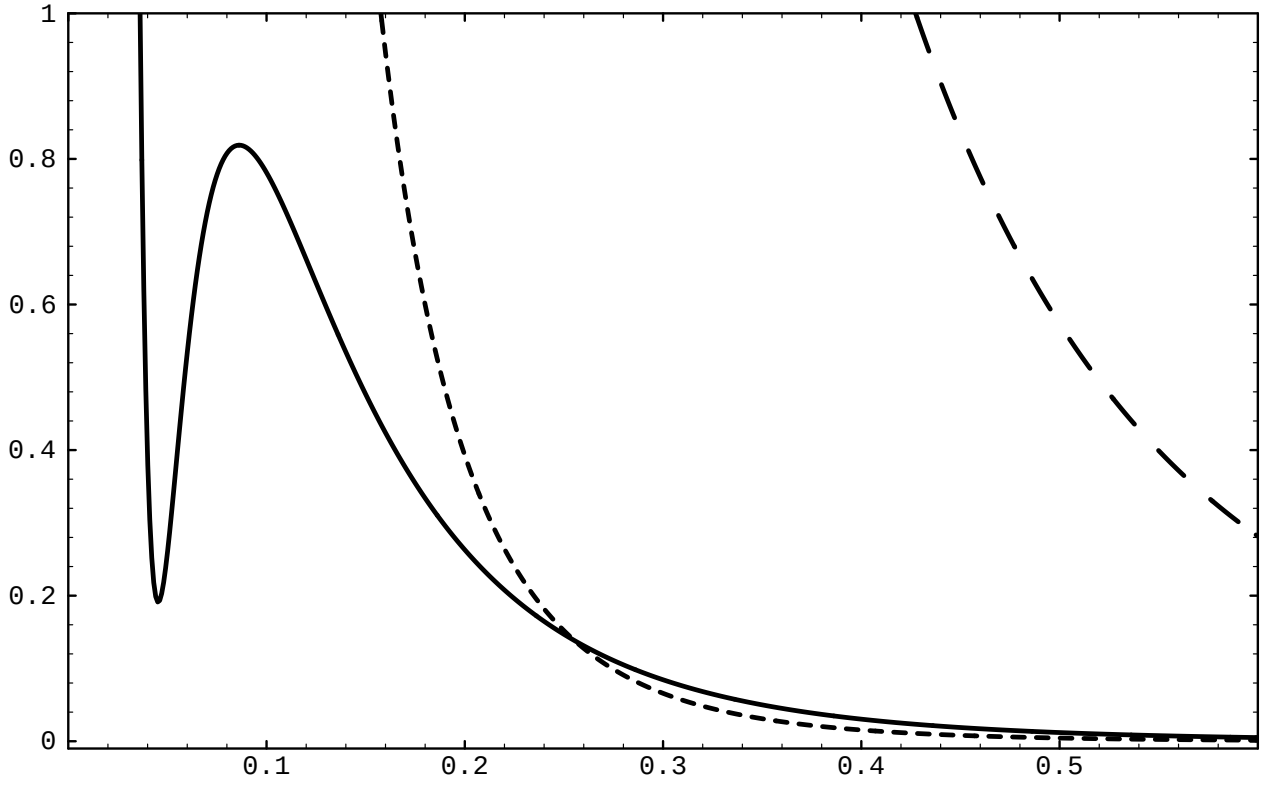

Figure 9

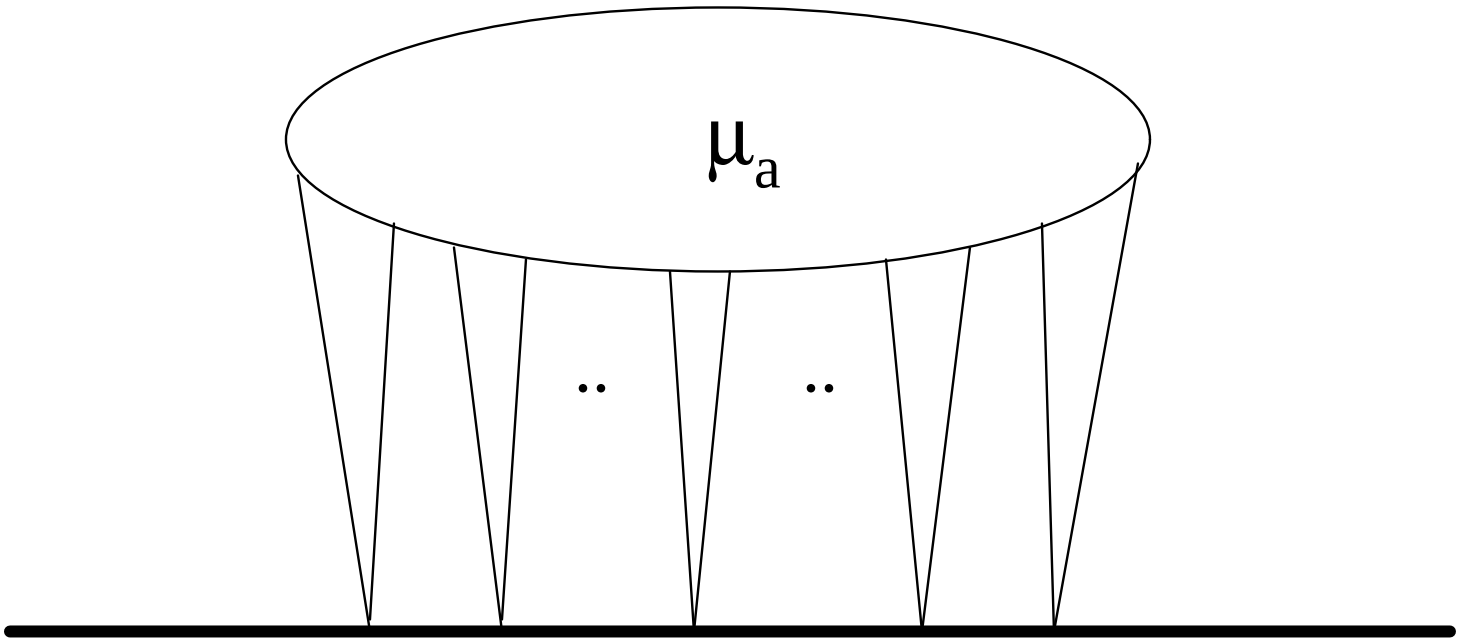

Figure 10

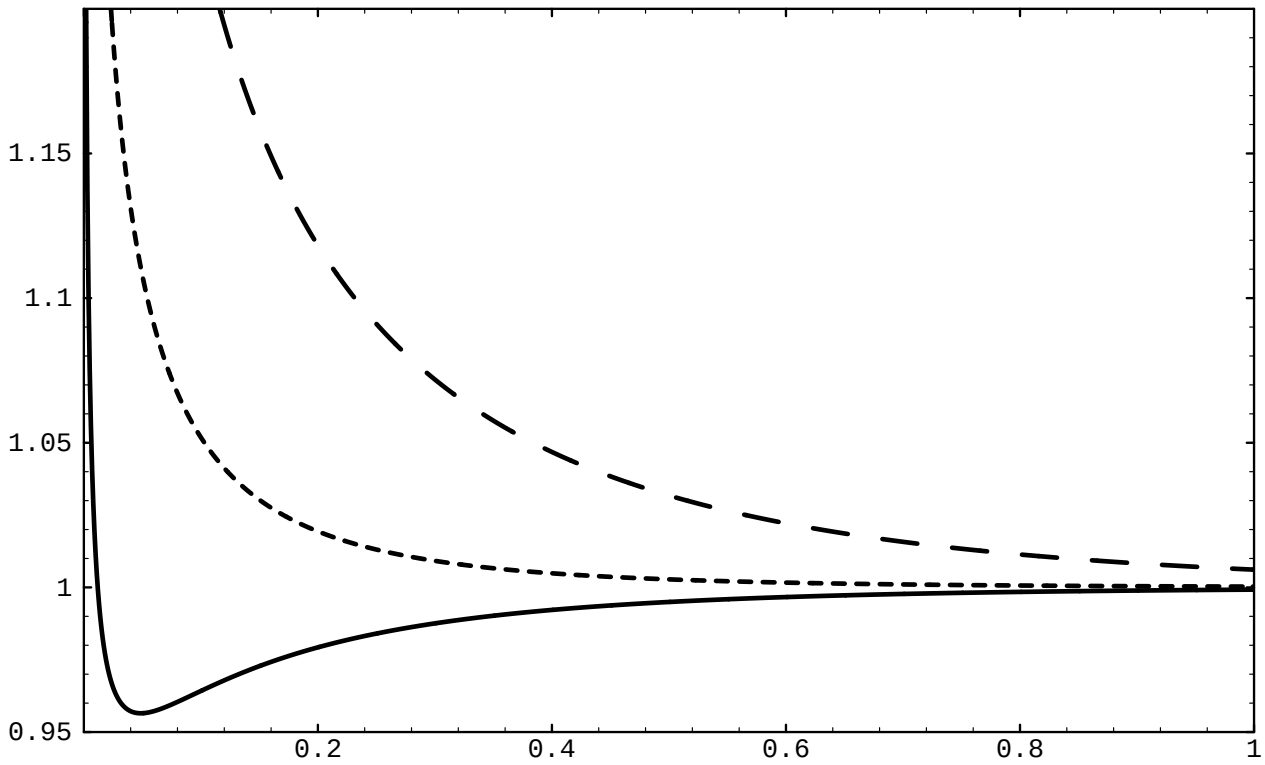

Figure 11

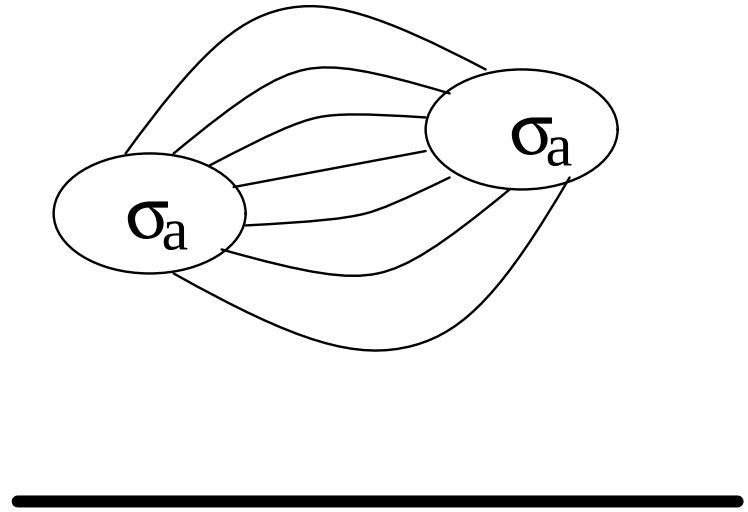

(a)

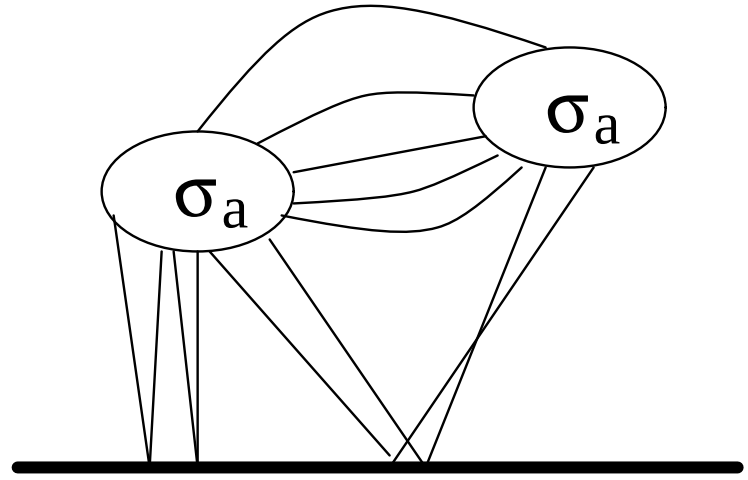

(b)

Figure 12

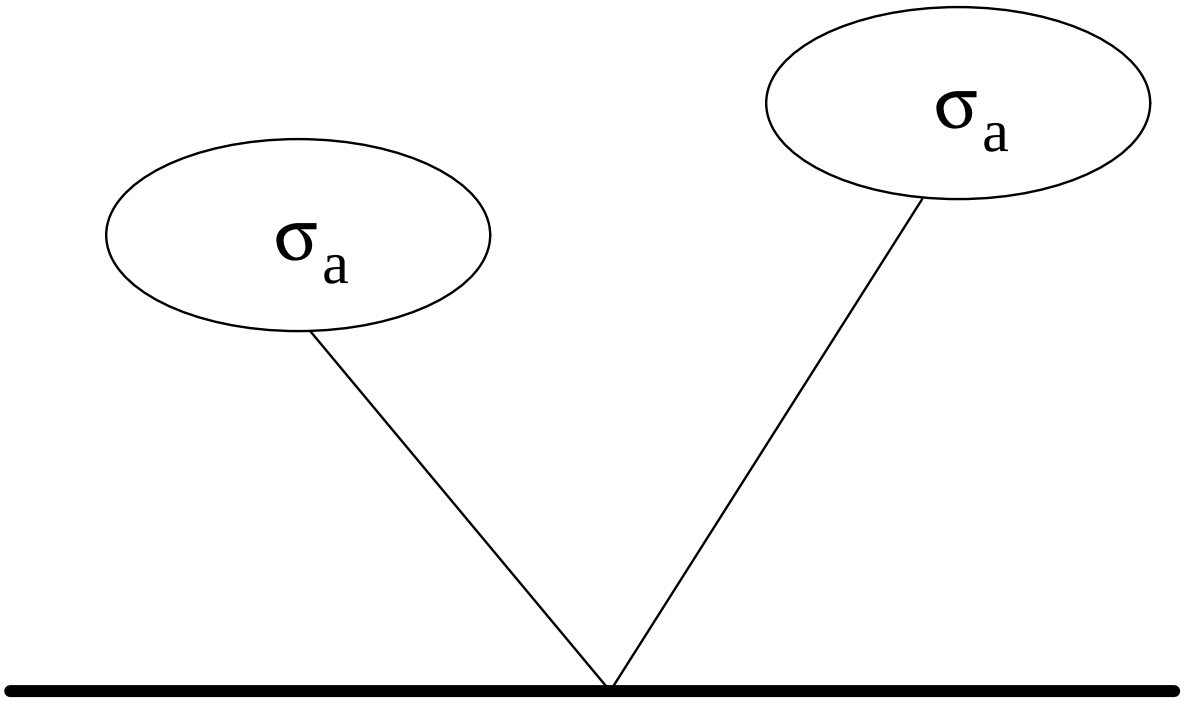

Figure 13

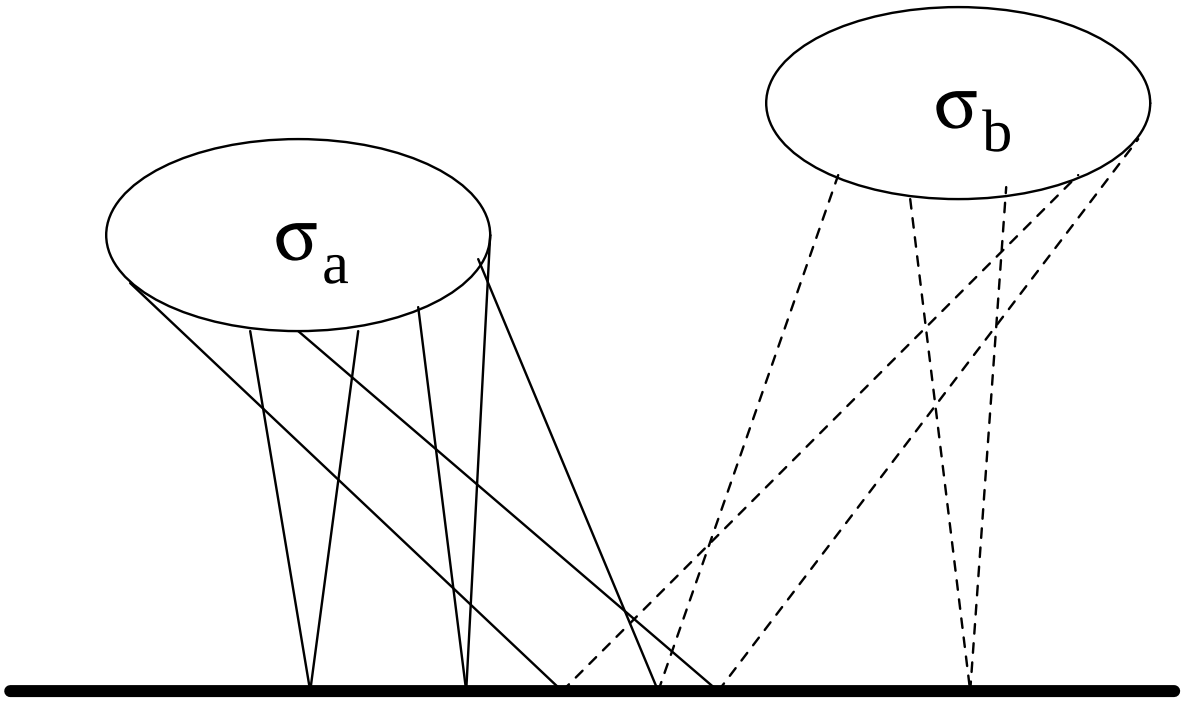

Figure 14

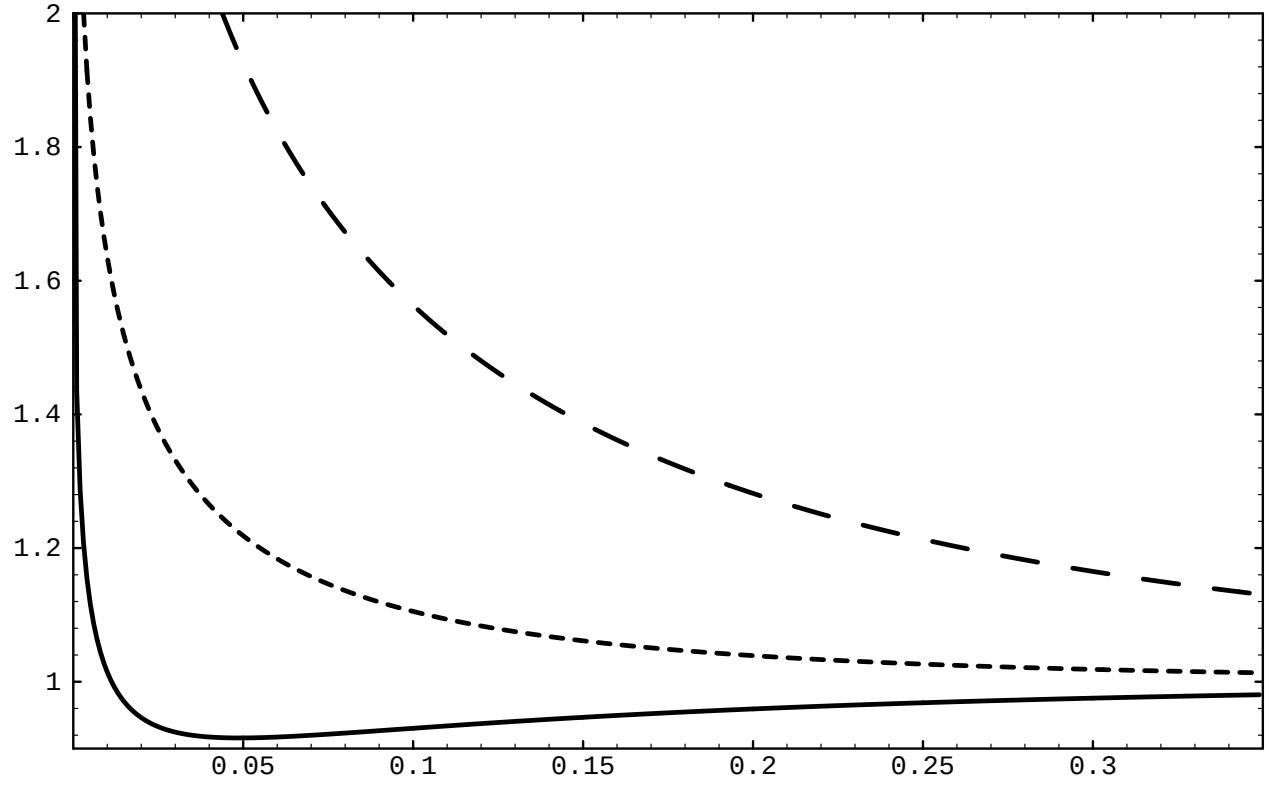

Figure 15

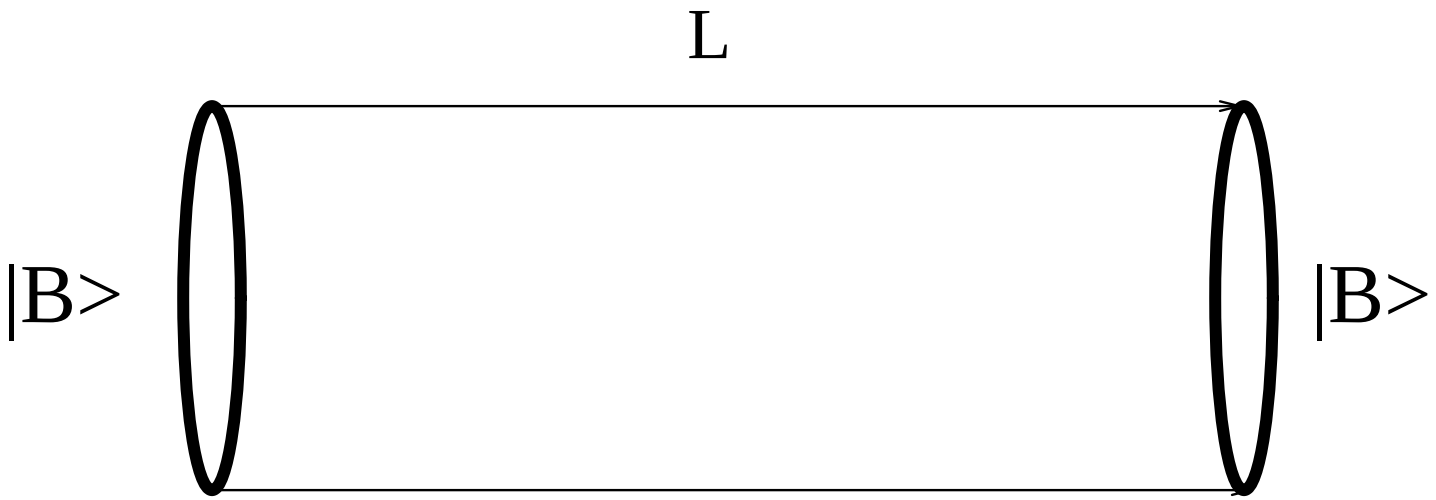

(a)

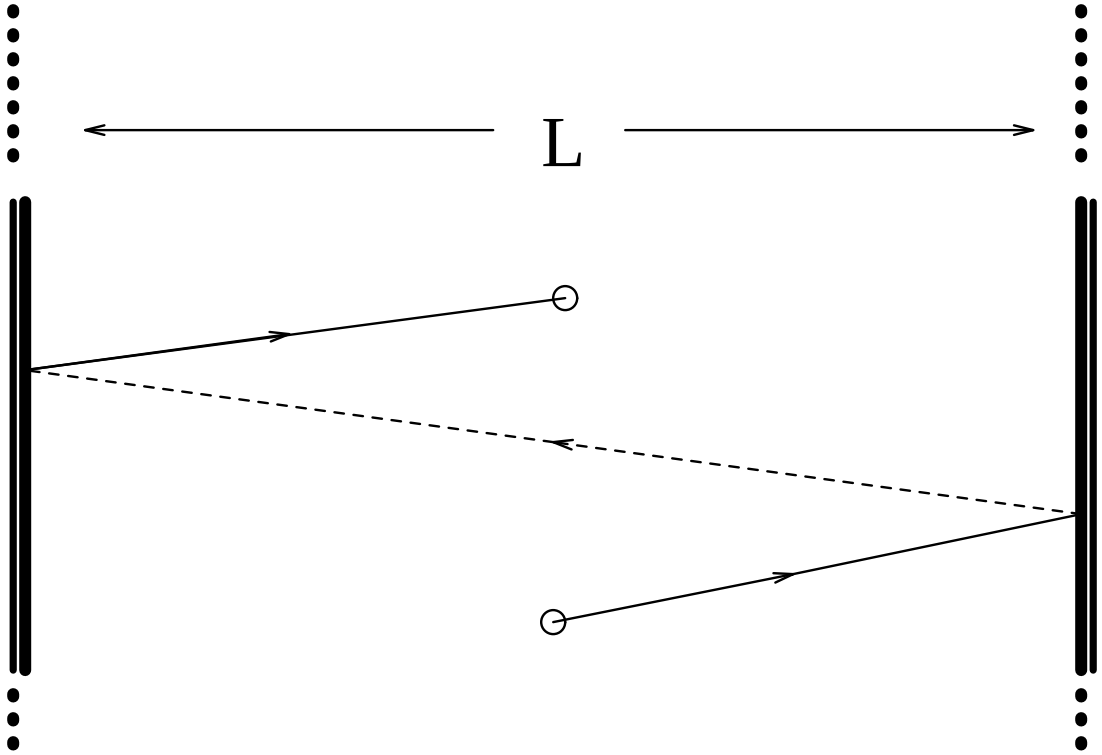

(b)

Figure 16